

Atoms in jellium

G. W. Bryant and G. D. Mahan

Physics Department, Indiana University, Bloomington, Indiana 47401

(Received 2 May 1977)

We report one-electron calculations of the soft-x-ray $L_{2,3}$ absorption and emission of Na, Mg, and Al and the soft-x-ray K absorption and emission of Li. The absorbing ion is placed at the center of a metal consisting of a valence band of electrons and of a uniform positive background which has a spherical hole removed from around the ion. Self-consistent solutions for states with and without a core hole are found using the density-functional approach. However, we eliminate self-interaction effects from the bound-state wave equation in order to get more realistic wave functions. This was originally proposed by Cowan but ignored subsequently. We think it is essential for getting good wave functions. In our solution both the core electrons bound to the central ion and the valence electrons are allowed to relax into the self-consistent solution. We find self-consistent potentials, charge densities, and threshold energies for soft-x-ray transitions. Scattering states in the relaxed potentials are used in spectrum calculations. We report cross sections found for Li, Na, Mg, and Al and compare them with experimental results. Moreover, we calculate the exponents α , α_0 , and α_1 essential to the threshold theory of Mahan and Nozières and de Dominicis (MND). For Li, Mg, and Al we get agreement with experimental results for α and α_0 . We get no agreement for Na but we attribute this not to a failure in MND theory but to an inadequacy in our model when used to find low-energy zero-angular-momentum valence-electron wave functions.

I. INTRODUCTION

The density-functional formalism was introduced by Hohenberg and Kohn¹⁻³ nearly 15 years ago to investigate systems with an inhomogeneous electron density. Combined with the Kohn-Sham local-density approximation for the exchange energy,^{3,4} it provides a simple straightforward method for finding a self-consistent single-particle potential which includes electron-electron interactions. With this formalism there is no need to use pseudopotentials or make other approximations to the potential.

The density-functional formalism has been used with much success to study the ground-state properties of electron systems. When applied to atoms⁵⁻¹¹ the density-functional method works very well, especially considering that the charge density varies rapidly in an atom. Threshold energies for photoionization can be obtained that agree with Hartree-Fock results. Spectra for photoionization can also be obtained. When applied to metals the density-functional method again works well. When combined with an augmented-plane-wave (APW) calculation¹²⁻¹⁶ good results for band structure are obtained. Tong¹⁷ used the formalism in a modified cellular method to calculate compressibility. Dagens¹⁸ calculated the displaced charged density around a completely screened ionic potential using the auxiliary neutral-atom method. Almladh and others have studied the nonlinear effects of the screening charge induced around a point-charge impurity.^{19,20} The density-functional method has also been used to study the electron

structure near metal surfaces.^{2, 21-23} Surface potentials, charge densities in the region near the surface, and surface energies are calculated.

The density-functional method is rigorously applicable only to the study of the ground-state properties of systems with a nondegenerate ground state. However, under the assumption that the core hole created during a soft-x-ray transition can be treated as a weak external potential, Almladh and von Barth²⁴ have treated the excited state created in x-ray absorption using the density-functional method. Their calculations for absorption thresholds agree with experiment. Flynn and Lipari²⁵ used a modified form of the density-functional method and also obtained good agreement with experiment for their threshold-energy calculations.

Soft-x-ray absorption and emission in metals involve transitions between the ground state of the metal and an excited state with one-core hole. Most calculations of soft-x-ray emission and absorption²⁶⁻²⁸ either use some approximation for the potential to describe the scattering of the ejected electron or assume that the ejected electron moves in the potential of the ground state. Ritsko, Schnatterly, and Gibbons²⁶ include final-state interactions by using plane waves orthogonalized to the final-core states. They include band-structure effects by including backscattering from near neighbors, but they use approximate core-wave functions. Gupta and Freeman²⁷ also include band-structure effects in their calculation of Mg spectra by making a careful APW calculation to find matrix elements and a detailed density of states.

Smrcka²⁸ makes a similar calculation for Al. In each case electron wave functions are calculated using methods appropriate to study the ground state. This is not necessarily an adequate approximation. The valence electrons screen the core hole created during the absorption in a time ω_p^{-1} where ω_p is the plasmon frequency. In metals ω_p^{-1} is about 10^{-15} sec. An electron with energy near the Fermi energy (velocity about 2×10^8 cm/sec) does not travel away from the range of the core potential in that time. For that reason one should use the excited-state wave functions in calculating absorption spectra. In calculating emission spectra one must use the electron wave functions when the core hole is present because this is the initial state. The formalism commonly used to study ground-state properties in metals—APW, orthogonalized-plane-wave (OPW), the cellular method, etc.—all use the translation symmetry of the metallic ground state. They are not so useful for studying a metal with a core hole because the core hole destroys the translation symmetry. However the density-functional method has proved successful in studies of both the ground state and the core-hole state and is thus better suited for use in calculations of absorption and emission spectra.

In this paper we use the density-functional approach to study the ground-state properties of simple metals and the properties of simple metals with a core hole. We calculate soft x-ray spectra for both emission and absorption. By comparing our single-particle calculations with the extensive experimental observations²⁹⁻³³ we find out where many-body and band-structure effects are needed to explain the structure of soft-x-ray spectra. Moreover, since we calculate electron wave functions for the metal with and without a core hole, we determine the phase shifts for electrons scattering off the core hole. This allows us to test the theoretical predictions of Mahan,³⁴ Nozières and de Dominicis,³⁵ and Doniach and Sunjic³⁶ for exponents α , α_0 , and α_1 , that describe the anomalous power-law behavior of spectra near threshold, by comparing our calculations for the exponents with values extracted from soft-x-ray experiments^{37, 38} and XPS measurements.^{39, 40}

To use the density-functional method we must have a model for a metal. In Sec. II we describe our model. We treat the other ions as a uniform positive background. Around the central ion, which undergoes the transition, we remove a sphere of charge from the positive background. Thus we have no background charge in the sphere around the central ion. We find wave functions for all the valence electrons and the electrons bound to the central ion. We use the density-func-

tional formalism to obtain single-particle equations describing the electrons. We use the Kohn-Sham local-density approximation for the exchange energy and the Wigner form for the correlation energy.⁴¹ However, we make one significant change in our application of the density-functional formalism. The Coulomb potential used in the density-functional formalism has self-interaction effects that should be cancelled by the exchange potential but are not when it is approximated by the Kohn-Sham local-density exchange. For valence electrons this is a negligible effect, but for bound electrons self-interaction makes a major contribution because the bound electron is localized and makes a large contribution to the charge distribution near the core. To eliminate this effect we subtract the self-interaction from the potential we use in the single-particle equation for bound states. Although this correction was originally proposed by Cowan⁴² for atoms it has been ignored in applications of the density-functional method.

Almbladh and von Barth²⁴ recently presented a model similar to ours. They include a background that is more realistic by taking it as a certain spherical average of the real background. They use the density-functional approach but they do not make our self-interaction correction. They predict α , α_0 , and α_1 as well as threshold energies. They get good agreement for the energies but their values for α and α_0 do not always agree with experiment. They are not completely optimistic about the ability of the theory of Mahan, Nozières, and de Dominicis (MND) to predict exponents. Their poor value of α_0 for Al is responsible for much of their pessimism.

Flynn and Lipari²⁵ also studied the threshold properties of simple metals but they predicted only threshold energies. They used a modified self-consistent-field method and pseudopotentials to describe valence-electron interactions with the background. They were able to calculate threshold energies in agreement with experiment but they did not find valence-electron wave functions and so were unable to make any calculations of α , α_0 , α_1 , or spectra.

In Sec. III we present our results for free ions. We predict photoionization thresholds of Ne, Na⁺, Mg²⁺, and Al³⁺ with only 1% error. We also calculate photoionization cross sections for Ne. When we include self-interaction effects we get very poor results. When we exclude these effects we get much better agreement with the measurements of Samson⁴³ and Hartree-Fock theories.⁴⁴ This gives us confidence that we can treat core effects adequately by our method at least for ten electron ions.

In Sec. IV we present our results for metallic Li, Na, Mg, and Al. We predict threshold energies for the soft-x-ray transitions of Li, Mg, and Al with only 2%–5% error. We find this to be very satisfactory. We find the energies as the difference between the energies of the core-hole state and the ground state using the energy functional of the density-functional method and make no attempt to include additional corrections. Our result for Na is not as good because our solution for the Na-2*p* core-hole state shows bound-state resonances in the valence band not observed in experiments. We also present potentials and phase shifts for metal states with and without a core hole. The potentials are short range and screened as one would expect. In addition, we present charge densities of core and valence electrons. We find very little perturbation of the valence band when there is no core hole. With a core hole there is a screening charge of electrons just outside the core.

We also present the single-particle cross sections both in the normal approximation and the sudden approximation. In the normal approximation the wave function of the outgoing valence electron is calculated with a potential that has the system relaxed in its final state with a core hole. In the sudden approximation the final-state wave function is computed using the initial potential. We find similar results in absorption for both approximations. When we compare our calculations to experimental spectra³⁹ for Mg and Al we get good qualitative agreement but we cannot reproduce the structure. We also find that the ratio σ of *s*-wave cross section to *d*-wave cross section at threshold is greater than one for Na and Mg and about one for Al. This is a change from the free-ion result that σ is small and confirms the experimental fact that *s*-wave effects are dominant near threshold in many metals. We also present emission results for Li, Na, Mg, and Al. However we get poor agreement with experiment³⁰ for Na, Mg, and Al. For these metals our results predict low-energy peaks indicative of *s*-wave resonances. However these are not observed experimentally.

We make calculations of α , α_0 , and α_1 for each metal. We get good agreement with experiments for many of the exponents. This gives us confidence in the power of MND theory. However the indications of a bound state seen in the emission cross section for Na carry over to the Na phase shifts. As a result we get values for the exponents that differ considerably from experiment. This failure is an artifact of our model and cannot be attributed to MND theory.

II. THE MODEL

We want to describe the situation in which the disturbance in a metal due to a particular ion,

either an impurity or a host ion undergoing an optical transition, does not extend too far from the ion itself. The valence electrons are able to screen the disturbance within several lattice spacings and outside this region the potential is weak. Except for Friedel oscillations the metal remains unperturbed by the disturbance and is nearly uniform everywhere. The simplest model for a metal is the jellium model with a valence band of electrons and a uniform positive background made from the nuclear charges and the core electrons bound to them. The charge density of the background is fixed to neutralize the charge of the valence electrons. This is the model we consider.

The ion under consideration is placed at the center of the metal. Because we start from ionic ground states that are closed shells and thus spherically symmetric (i.e., Li⁺, Na⁺, Mg²⁺ or Al³⁺) the disturbance in the jellium environment is spherically symmetric. When a core hole is created this symmetry is broken. However we assume this is a small effect. Thus we always consider a system in which charge densities have been spherically averaged, as in the restricted Hartree-Fock method.

In a realistic model of the metallic environment of the ion under consideration, the positive background should not extend to the ion's nucleus. For that reason we delete a sphere of charge from the positive background that surrounds the ion. The radius of the sphere r_{ws} is just the Wigner-Seitz radius—the radius corresponding to the volume of one atom in the metal (see Table II). We treat the positive background with the hole and the nucleus of charge Z at the center of the hole as a fixed external potential. Within this potential we allow the core electrons bound to the central nucleus and all the valence electrons to interact, relax, and screen any disturbance.

Because we consider a uniform background and take our system to be spherically symmetric we lose all band-structure effects in our calculation and the density of states is taken to be spherically symmetric. Moreover, because the perturbing potential decays quickly, the valence-electron density is uniform almost everywhere and the Fermi energy is left unchanged. Thus the density of states for the valence electrons is the same as that for free electrons in the jellium model.

With this model we study the soft-x-ray absorption and emission. We first find a self-consistent solution with wave functions for the core and valence electrons when there is no core hole. For Na, Mg, and Al we then find a self-consistent solution for the state with one 2*p* core electron excited to a state at the Fermi level. For Li we find

a self-consistent solution for the 1s core hole state. The valence states used in calculating transition matrix elements are obtained using the potential due to electrons fully relaxed around the core hole. In doing this we assume that core and valence electrons relax quickly enough so that the outgoing electron moves in this fully relaxed potential. For emission calculations this is the correct procedure because the initial state is this fully relaxed and screened core-hole state. For absorption we also calculate transition-matrix elements in the sudden approximation in which the outgoing electron wave function is calculated with the potential of the state without a core hole. We can then compare these two approximations for finding the transition-matrix elements.

To calculate these matrix elements we need the valence and bound-state wave functions. We find these by using the single-particle equation obtained by the density-functional method,¹⁻³

$$\left(-\nabla^2 - \frac{2Z}{r} - 2 \int d^3r' \frac{n(\vec{r}') - \rho(\vec{r}')}{|\vec{r} - \vec{r}'|} + V_{\text{ex}}(\rho(\vec{r})) + V_{\text{cor}}(\rho(\vec{r})) \right) \psi_i(\vec{r}) = \epsilon_i \psi_i(\vec{r}), \quad (1)$$

where Z is the nuclear charge, $n(\vec{r})$ is the charge density of the positive background,

$$n(\vec{r}) = \begin{cases} \frac{k_F^3}{3\pi^2} & \text{if } r > r_{\text{WS}} \\ 0 & \text{if } r \leq r_{\text{WS}}, \end{cases}$$

and

$$\rho(\vec{r}) = \sum_{\text{bound states}} |\psi_i(\vec{r})|^2 + \sum_{\text{valence states } \epsilon < \epsilon_F} |\psi_i(\vec{r})|^2.$$

All energies are measured in rydbergs and lengths are measured in Bohr radii. We approximate the exchange potential by the Kohn-Sham local-density exchange potential

$$V_{\text{ex}}(\rho(\vec{r})) = -2[(3/\pi)\rho(\vec{r})]^{1/3}.$$

We use Wigner's results for the correlation potential

$$V_{\text{cor}}(\rho(\vec{r})) = \frac{\delta}{\delta\rho} [\epsilon_{\text{cor}}(\rho(\vec{r}))\rho(\vec{r})],$$

where

$$\epsilon_{\text{cor}}(\rho(\vec{r})) = \frac{-0.88}{(3\rho(\vec{r})/4\pi)^{1/3} + 7.8}.$$

We use this as a simple approximation for what should be a small effect.

We actually use Eq. (1) only for the valence-electron wave functions. To find the bound-electron wave functions we use another, more realistic wave equation. When the Kohn-Sham exchange en-

ergy is used to approximate the Hartree-Fock exchange energy,⁴ the Coulomb self-energy for the electrons is included in the exchange term. To cancel that addition, the Coulomb self-energy is also included in the direct electrostatic energy. When the exchange energy is approximated by the Kohn-Sham local-density exchange potential these self-interaction effects no longer cancel. For a free atom the Coulomb plus exchange potential vanishes at large distances from the atom. For a bound electron this is a poor approximation to the $-2/r$ potential that a bound electron moves in far from the nucleus. When we calculate valence states in a metal we do not worry about the inclusion of the self-interaction because it has an effect of order $1/N$ ($N \sim 10^{22}$) on the potential and is negligible. However, the effect of the direct self-interaction of a bound electron on the potential is at least $1/Z$ near the nucleus where the bound-electron wave function is sensitive to the form of the potential. The bound-electron self-interaction should not be kept in the potential used for calculating the wave function of that electron. Similarly we should correct the exchange term but, because it varies as $[\rho(\vec{r})]^{1/3}$, any change in $\rho(\vec{r})$ will not make a large change in the exchange term. Cowan⁴² also suggested this self-interaction correction in his study of atoms. In addition, he parameterized the exchange potential by requiring that the virial theorem be satisfied, that the energy eigenvalues be the binding energies and that there be no exchange energy for orbitals occupied by one or two electrons. This procedure is not readily applicable to our model because we must include core-valence electron interactions and valence-valence electron interactions as well as core-core electron interactions. Rather than make an *ad hoc* change in the exchange term we leave it as it is. For bound states we use the wave equation

$$\left(-\nabla^2 - \frac{2Z}{r} - 2 \int d^3r' \frac{n(\vec{r}') - \rho(\vec{r}') + |\psi_i(\vec{r}')|^2}{|\vec{r} - \vec{r}'|} + V_{\text{ex}}(\rho(\vec{r})) + V_{\text{cor}}(\rho(\vec{r})) \right) \psi_i(\vec{r}) = \epsilon_i \psi_i(\vec{r}). \quad (1')$$

With this modification the bound states are calculated using a more realistic potential. The charge density determined by these bound states will be more realistic as will the Coulomb potential calculated using the core charge density. Since the valence electrons interact with the core electrons, this improvement will affect the valence wave functions as well.

We obtained self-consistent solutions using this formalism by employing a modified Herman-Skillman program.⁵ We calculate only valence wave

functions for s , p , d , and f states. Higher angular-momentum states are only slightly perturbed and we use free-electron wave functions for these states. At large distances from the ion we cannot find the electron density accurately by numerical means. By calculating phase shifts for valence states we determine the correct asymptotic expression for $\rho(\vec{r})$ and we include its effects in the Coulomb potential. In this manner we get the Friedel oscillations that one would expect around an impurity.

We first used the iterative procedure of Herman and Skillman to get self-consistent potentials and wave functions. In their procedure one first chooses a starting potential. This is used to generate new wave functions and a new potential. A suitable average of the two potentials is taken as the next starting potential. This iteration procedure is continued until the starting potential and the potential it generates are sufficiently self-consistent. For free ions this procedure is very successful and self-consistency is obtained quickly. For our model this procedure is not enough. If the starting potential generates a charge density that does not give a neutral system, then instabilities are introduced into the iteration procedure that are sufficient to prevent getting adequate self-consistency. Following a suggestion of Zaremba *et al.*²⁰ we modified our convergence procedure. After each iteration step we form a new potential with a value at each point which is between the values at that point of the starting and final potentials of the previous step. We then vary this new potential between the limits of the two previous potentials until we find one that obeys the Friedel sum rule. We take this potential to be our new starting potential. With this addition to our convergence procedure we are able to get self-consistent solutions which obey the Friedel sum rule to five decimal places. In the core region the difference between starting and final potentials is typically 0.005 Ry or less. In the asymptotic region where the potential becomes totally screened the difference is much less.

The model proposed by Almbladh and von Barth²⁴ differs from ours in several aspects. They do not make the self-interaction correction for bound states that we make. This can have a dramatic ef-

fect on calculated absorption cross sections, as our calculations for atomic Ne show. Although this correction primarily affects the bound-state wave functions, it can, through the charge density and the potential, affect the valence states. So we must be extremely careful in constructing the potential.

The model of Almbladh and von Barth also differs from ours in the choice of exchange and correlation potentials. The effects of both exchange and correlation are small compared to the Coulomb potential. The exchange potential is about -0.3 – -0.4 Ry. The correlation energy lowers the energy by 0.1 Ry. However in the region where the Coulomb potential decays to zero these other potentials are important. For Al we get similar results when we use potentials with and without Wigner correlation. It is not clear what is the best approximation for the exchange and correlation potentials.

We must find the energy of states with and without a core hole to find threshold energies. The starting point of the density-functional approach is the assumption that the energy of the system can be written as a functional of the electron density. In our model this functional takes the form

$$E(\rho) = \sum_{\text{occupied states}} \left(- \int \psi_i^*(\vec{r}) \nabla^2 \psi_i(\vec{r}) d^3r \right) - 2Z \int d^3r \frac{[\rho(\vec{r}) - n(\vec{r})]}{r} + \int \frac{[n(\vec{r}) - \rho(\vec{r})][n(\vec{r}') - \rho(\vec{r}')]}{|\vec{r} - \vec{r}'|} d^3r d^3r' + \int [\epsilon_{\text{ex}}(\rho(\vec{r})) + \epsilon_{\text{cor}}(\rho(\vec{r}))] \rho(\vec{r}) d^3r, \quad (2)$$

where

$$\epsilon_{\text{ex}}(\rho(\vec{r})) = -\frac{3}{2} [(3/\pi)\rho(\vec{r})]^{1/3}.$$

We use the variational principle derived by Hohenberg and Kohn to obtain Eq. (1) from Eq. (2). To find the energy of the system we use Eqs. (1) and (1') to evaluate the first term in Eq. (2). We find that

$$E(\rho) = \sum_{\text{bound states}} \epsilon_i + \sum_{\text{valence states } \mathbf{k} < \mathbf{k}_F} \int k^2 |\psi_{\mathbf{k}}(\vec{r})|^2 d^3r + 2Z \int d^3r \frac{n(\vec{r})}{r} + \int \frac{[n(\vec{r}) - \rho(\vec{r})][n(\vec{r}') + \rho(\vec{r}')]}{|\vec{r} - \vec{r}'|} d^3r d^3r' - \int \frac{\delta}{\delta \rho} [\epsilon_{\text{ex}}(\rho(\vec{r})) + \epsilon_{\text{cor}}(\rho(\vec{r}))] \rho^2(\vec{r}) d^3r + 2 \sum_{\text{bound states}} \int \frac{|\psi_i(\vec{r})|^2 |\psi_i(\vec{r}')|^2}{|\vec{r} - \vec{r}'|} d^3r d^3r', \quad (3)$$

where the energy eigenvalue of Eq. (1) for a valence state ψ_k is k^2 . We note that the last term in Eq. (3) is the correction we must include because the self-interaction term is excluded in Eq. (1'). We also note that in our model the jellium has infinite extent and thus several terms in Eq. (3) are infinite. By subtracting from Eq. (3) those energy contributions that a system with a uniform valence band would make we get an energy expression that gives a finite result.

III. FREE-ION RESULTS

We first checked our method by calculating photoionization cross sections and threshold energies for the free-ion transitions $\text{Ne} \rightarrow \text{Ne}^+$, $\text{Na}^+ \rightarrow \text{Na}^{2+}$, $\text{Mg}^{2+} \rightarrow \text{Mg}^{3+}$ and $\text{Al}^{3+} \rightarrow \text{Al}^{4+}$. These are all transitions from ten electron closed-shell states to nine electron $2p$ -hole states. Threshold energies have been accurately computed before, beginning with Tong and Sham.⁶ We have similar success. Using Kohn-Sham exchange we get ionization energies that are about 0.09 Ry too low—an error of 2%–5% (see Table I). Correlation effects²⁵ cause this systematic error. When we include Wigner correlation (see Table I) the error is only 0.01 Ry or less than 1%. We also calculated threshold energies using Slater exchange but the values computed were all too big. Slater exchange makes the potential too attractive and the extra electron is too tightly bound. However, the threshold energies are much less sensitive to whether or not we make the self-interaction correction to the bound-electron wave equations. We also calculated the threshold energy for $\text{Li}^+ \rightarrow \text{Li}^{++}$. For Li the agreement with experiment is poor because we include exchange effects that do not exist for one and two electron ions. Although we cannot use our model for free Li ions, we can use it for metallic Li because there are exchange interactions between electrons in the valence band.

We calculated the cross section for each photoionization transition mentioned above. In each

TABLE I. Calculated and experimental threshold energies for photoionization from the indicated ion ground state. E_{ex} includes exchange effects. $E_{\text{ex-cor}}$ includes correlation as well as exchange effects. The experimental values E_{exp} are taken from the work of Moore (Ref. 45).

(Rydbergs)	Ne	Na ⁺	Mg ²⁺	Al ³⁺
E_{ex}	1.50	3.39	5.80	8.73
$E_{\text{ex-cor}}$	1.59	3.48	5.89	8.81
E_{exp}	1.58	3.48	5.89	8.82

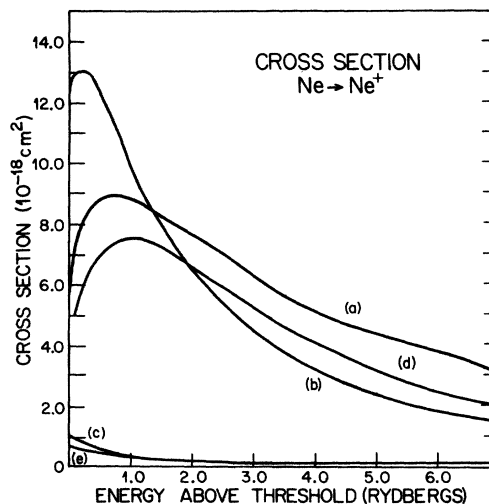


FIG. 1. Experimental and theoretical calculations for the photoionization cross section of free Ne: (a) the experimental measurements of Samson (Ref. 43), (b) the $2p \rightarrow d$ cross section when self-interaction contributions to the potential are included, (c) the $2p \rightarrow s$ cross section when self-interaction contributions to the potential are included, (d) the $2p \rightarrow d$ cross section when there is no bound-electron self-interaction, and (e) the $2p \rightarrow s$ cross section when there is no self-interaction.

case we computed the dipole approximation to the transition-matrix element using the length form for the matrix element. In the one-electron approximation the cross section for a transition with the outgoing electron changing its angular momentum from l to $l \pm 1$ is

$$\sigma_{l \rightarrow l \pm 1} = C_{l \pm 1} \xi (\hbar\nu/k) |\langle \psi_{k, l \pm 1} | r | \psi_{nl} \rangle|^2 \delta(\epsilon_k + \epsilon_{\text{th}} - \hbar\nu), \quad (4)$$

where ϵ_{th} is the threshold energy, $\hbar\nu$ the photon energy, ϵ_k the energy of the ejected electron, ξ the overlap of the remaining electrons (about 0.95 for free ions but taken to be unity for metals), ψ_{nl} is a bound-state wave function of angular momentum l , $\psi_{k, l \pm 1}$ is the continuum state with momentum k and angular momentum $l \pm 1$, and

$$\psi_{k, l \pm 1} \xrightarrow{r \rightarrow \infty} \frac{\sin}{r} \left(kr + \delta_l - \frac{l\pi}{2} \right) \quad \text{in metals,}$$

$$\psi_{k, l \pm 1} \xrightarrow{r \rightarrow \infty} \frac{\sin}{r} \left(kr - \frac{l\pi}{2} + \frac{Z}{k} \ln(2kr) + \eta_l + \delta_l \right),$$

for free ions, where $\eta_l = \arg[\Gamma(l+1 - iZ/k)]$ and δ_l is the phase shift.

The results for Ne, Mg^{2+} , and Al^{3+} are shown in Figs. 1, 4, and 5. In Fig. 1 we compare the experimental results of Samson⁴³ for the $\text{Ne} \rightarrow \text{Ne}^+$ cross section with our results. The $2p \rightarrow d$ and

$2p \rightarrow s$ transitions with and without self-interaction are shown. Near threshold dramatic improvement occurs when self-interaction effects are excluded. The $2p \rightarrow d$ plus $2p \rightarrow s$ cross section excluding self-interaction agrees well with the experimental observations. The discrepancy between the two methods is easy to understand. When self-interaction is included a core electron is repelled not only by the other core electrons but by its own charge distribution as well. Thus a core electron is less tightly bound when self-interaction is included. The overlap between the core wave function and the continuum wave function is then sufficient to give a large cross section even for low-energy d -wave electrons which are kept away from the ion by the centrifugal barrier. When the direct self-interaction is taken out, the electron is more tightly bound, the overlap with low-energy d -wave electrons decreases and the cross section is suppressed. The core wave functions differ by only 5% between the two approximations but this still leads to a 50% decrease in the cross section near threshold.

We find several interesting features when we consider the photoionization cross sections for $\text{Ne} \rightarrow \text{Ne}^+$, $\text{Mg}^{2+} \rightarrow \text{Mg}^{3+}$, and $\text{Al}^{3+} \rightarrow \text{Al}^{4+}$. The $2p \rightarrow s$ transition is strongest for Ne, weaker for Mg^{2+} , and weakest for Al^{3+} . The potential for Ne is the least attractive because Ne has the smallest nuclear charge. Thus the $2p$ electron in Ne is the least bound. This is reflected in the overlap integrals. They are largest for Ne and Ne has the largest $2p \rightarrow s$ cross section. In general the $2p \rightarrow d$ transitions also follow this pattern and for the same reason. However, near threshold the Na^+ cross section actually flattens out and the Ne cross section begins to decrease. Only the Mg^{2+} and Al^{3+} cross sections continue to rise towards threshold. The overlap integral is still largest for Ne but, for the $2p \rightarrow d$ transition, the frequency factor ν appearing in Eq. (4) controls the form of the curve near threshold. Near threshold, ν for Ne is half the ν for Na^+ while the overlap integrals are closer in magnitude. By using the relation⁴⁶

$$[H, r] = -i\hbar \frac{d\hat{r}}{dt} = -i\hbar \hat{v},$$

the length-matrix element is transformed to a velocity-matrix element

$$|\langle \psi_{k, i \pm 1} | \hat{r} | \psi_{n i} \rangle| \rightarrow (1/\nu) |\langle \psi_{k, i \pm 1} | \hat{v} | \psi_{n i} \rangle|.$$

Then

$$\sigma_{i \rightarrow i \pm 1} \sim \frac{1}{k\nu} \left| \langle \psi_{k, i \pm 1} | p_r | \psi_{n i} \rangle \right|^2,$$

where p_r is the radial momentum. Ne has the

least attractive potential so the centrifugal potential has the largest effect. The radial momentum of the low-energy continuum electrons should be small. This is reflected in the small cross section for Ne. In Al the potential is more attractive and the radial momentum matrix element is large enough that the cross section does not decrease near threshold. Finally, the $2p \rightarrow d$ transitions are stronger than the $2p \rightarrow s$ transitions. There are two reasons for this. First there are six allowed $2p \rightarrow s$ transitions. Furthermore the s states have nodes in the region where the bound state is finite, but low-energy d -wave states have no nodes in this region.

IV. METAL RESULTS

We present results for Li, Na, Mg, and Al. We obtain good self-consistent solutions for both the states with and without a core hole for each metal. In Table II we give the parameters used for each metal. Since we assume that the density of states is that of a free-electron model we use free-electron values for the Fermi momentum k_F and the Fermi kinetic energy ϵ_F .

In Table III we present calculations for the K soft-x-ray threshold energy in Li and the $L_{2,3}$ threshold energy in Na, Mg, and Al. Our results for Li, Mg, and Al differ from experiments only by 2%–5%. This is quite satisfactory because our results are just the difference in energies of the states with and without a core hole. We make no attempt to include any additional corrections. We note that our result for Li is satisfactory even though we cannot predict a threshold energy for Li^+ . Our model is not applicable to free Li ions because they have no exchange interactions. However, for metallic Li we get good results because there are exchange interactions between electrons in the valence band. Our result for Na is not as good as those for the other metals. Our solution for the $2p$ core-hole state of Na shows anomalous behavior that our other solutions do not show. There are resonances in the low kinetic-energy s -wave valence states. This affects the phase shifts and the energy calculation.

TABLE II. The Fermi momentum k_F , the Fermi energy ϵ_F , and the Wigner-Seitz radius r_{WS} .

	$k_F(a_0^{-1})$	ϵ_F (Ry)	$r_{\text{WS}}(a_0)$
Li	0.593	0.352	3.236
Na	0.487	0.237	3.941
Mg	0.720	0.518	3.358
Al	0.926	0.857	2.989

TABLE III. Experimental and theoretical values for threshold energies: (a) experimental results (Ref. 47), (b) calculations of Flynn and Lipari (Ref. 25), (c) calculations of Almbladh and von Barth (Ref. 24), and (d) this work.

Rydbergs	a	b	c	d
Li	4.02	4.08	4.08	4.09
Na	2.26	2.29	2.24	2.79
Mg	3.65	3.66	...	3.80
Al	5.36	5.35	5.35	5.29

In Fig. 2 we show the self-consistent potentials acting upon a valence electron in Al with and without a core hole. The results for the other metals are similar. In each case the potential is short range and screened. The metallic potentials are almost totally screened after one r_{ws} and are totally screened after two r_{ws} . The difference between potentials with and without a core hole is small showing that the $2p$ core hole is screened quickly and makes a small perturbation on the metal. We also see a very small bump in the potentials. This is typical of the potentials. The valence electrons screen the central potential too much. However the long-range Friedel oscillations in the charge density compensate this and the potential returns quickly to the asymptotic value $V_{ex}(\rho_0) + V_{cor}(\rho_0)$, where ρ_0 is the density of the unperturbed valence band.

We plot in Fig. 3 the excess radial-charge density for valence electrons [$4\pi r^2 \Delta\rho_v(r)$, where $\Delta\rho_v(r) = \rho_v(r) - \rho_0$ and $\rho_v(r)$ is the valence-charge density] and the radial-charge density for core

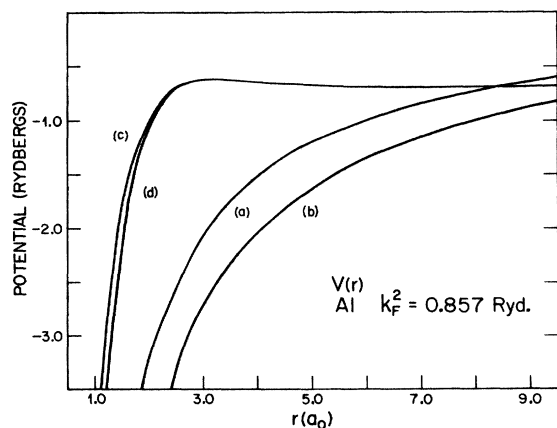


FIG. 2. Potentials seen by a continuum electron scattering off Al: (a) due to a free Al^{3+} ion, (b) due to a free Al^{4+} ion, (c) due to metallic Al without a core hole, (d) due to metallic Al with a $2p$ core hole.

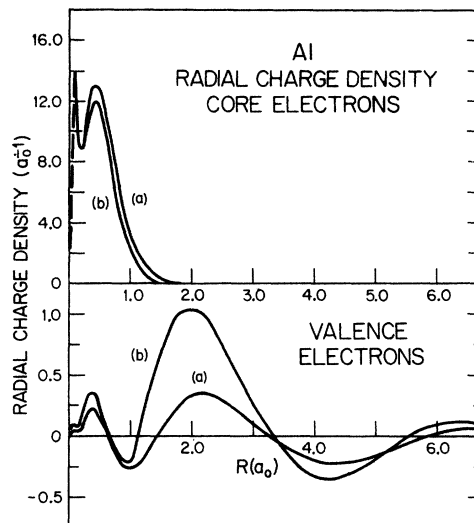


FIG. 3. Radial charge density of the core electrons and the excess valence electrons in metallic Al: (a) without a core hole, (b) with a $2p$ core hole. Note the change in scale for the core and valence-electron densities. r_{ws} is $2.99a_0$.

electrons. The valence electrons around a core hole bunch up just outside the core electrons. The screening charge in the core-hole state is pulled toward the center due to its attraction to the core hole and it has a large peak to screen the core hole. The charge density decays quickly to the Friedel oscillations. These dominate the excess charge after two r_{ws} . Near the core the valence-electron density has an oscillatory behavior. This results from the extra nodes that appear in the valence wave functions due to the scattering potential.

In Table IV we present the position and magnitude of the main peak of the screening charge in the core hole state. As expected, the screening charge in Al is pulled closest to the central ion and the peak is largest in Al. This happens because the Al^{4+} ion has the most charge to be screened and because Al is the densest of the four metals. We note that the screening charge in Li is pulled closer than that of Na even though in both cases the same charge must be screened.

TABLE IV. Position and magnitude of the main peak in the radial-charge density for the screening charge in the core-hole state.

	Li	Na	Mg	Al
Position (a_0)	2.35	3.10	2.30	1.95
Magnitude (a_0^{-1})	0.55	0.36	0.68	1.02

TABLE V. Phase shifts and Friedel sums for both the ground state and core-hole state. δ_l is the phase shift at zero wave vector. $\Delta\delta_l$ is the difference between phase shifts at the Fermi level and at zero wave vector. FS is the Friedel sum.

	δ_0	$\Delta\delta_0$	δ_1	$\Delta\delta_1$	δ_2	$\Delta\delta_2$	FS
Li ground state	π	-0.3367	0.0	0.1411	0.0	-0.0118	0.000 000
Li 1s core hole	π	0.2745	0.0	0.5114	0.0	-0.0363	0.999 993
Na ground state	2π	-0.1301	π	0.0234	0.0	0.0134	0.000 000
Na 2p core hole	3π	-2.2646	π	0.7069	0.0	0.1971	1.000 000
Mg ground state	2π	-0.1335	π	0.0559	0.0	0.0047	0.000 006
Mg 2p core hole	2π	0.3435	π	0.3965	0.0	0.0251	1.000 000
Al ground state	2π	-0.1327	π	0.1276	0.0	-0.0073	-0.000 005
Al 2p core hole	2π	0.2265	π	0.4742	0.0	0.0260	1.000 000

The Li ion has only 1s electrons bound to it. The Na ion has 1s, 2s, and 2p electrons bound to it. These extra electrons around a Na ion prevent the valence electrons from getting as close to the center as those in Li.

In Table V we present phase shifts for the valence states at zero wave vector for both the core-hole state and the ground state. The phase shifts at zero wave vector are either zero or a multiple of π . For each multiple of π the wave function has one more node than the same wave function for a free electron. Except for the s-wave phase shift in the core-hole state of Na, the zero wave vector phase shifts of Na, Mg, and Al show the same characteristics. The s-wave phase shifts are 2π , the p-wave phase shifts are π , and all others are zero. The fact that δ_0 and δ_1 are not zero is indicative of the bound-state character of the s and p waves. The s waves show 3s bound-state characteristics, the p waves have 3p characteristics. This shows up in the emission cross sections as we will discuss. For d waves and higher angular momenta we have no resonant behavior because the centripetal potential keeps the electrons away from the core. The phase shifts for Li show the same trend but only the s-wave shift shows resonant characteristics.

We also show in Table V the change in phase shift in going from the zero wave vector state to the Fermi level. The s wave in the ground state is pushed out slightly and the p wave is pulled in slightly. Using the Friedel sum rule⁴⁸

$$\Delta\rho_v = (2/\pi) \sum_l (2l+1) \Delta\delta_l,$$

we find the amount of excess charge in the valence band. For the ground states $\Delta\rho_v$ is zero. In the ground state the s band loses a small amount of charge and the p band gets a compensating amount of charge. The d and higher bands are perturbed only slightly. In the core hole states the change in both the s- and p-wave phase shifts is positive.

Both bands gain an excess of charge. This is the charge that screens the core hole. Again the perturbation of the d band is small and exists primarily to insure exact-charge neutrality. The only strange behavior is seen in the phase shifts of the Na core-hole state. Because there is a resonance in the s-wave states the s band actually loses charge. To screen this loss and the core hole the perturbations in the p and d bands are much larger. This is another indication of how the reso-

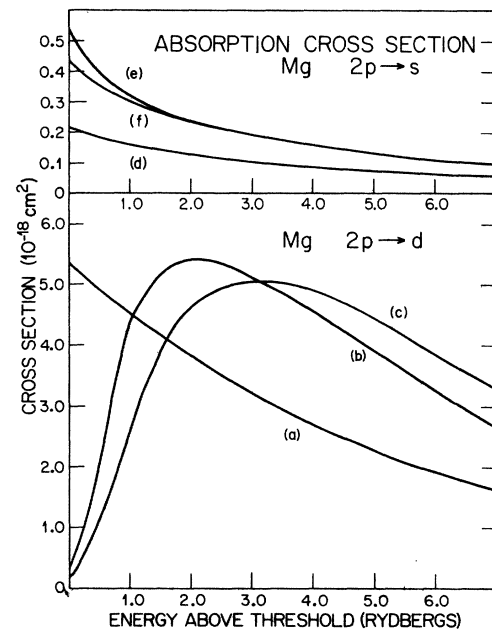


FIG. 4. $2p \rightarrow s$ and $2p \rightarrow d$ absorption cross section for Mg: (a) $2p \rightarrow d$ free Mg^{2+} ion absorption, (b) $2p \rightarrow d$ metallic Mg absorption in normal approximation, (c) $2p \rightarrow d$ metallic Mg absorption in sudden approximation, (d) $2p \rightarrow s$ free Mg^{2+} ion absorption, (e) $2p \rightarrow s$ metallic Mg absorption in normal approximation, and (f) $2p \rightarrow s$ metallic Mg absorption in sudden approximation.

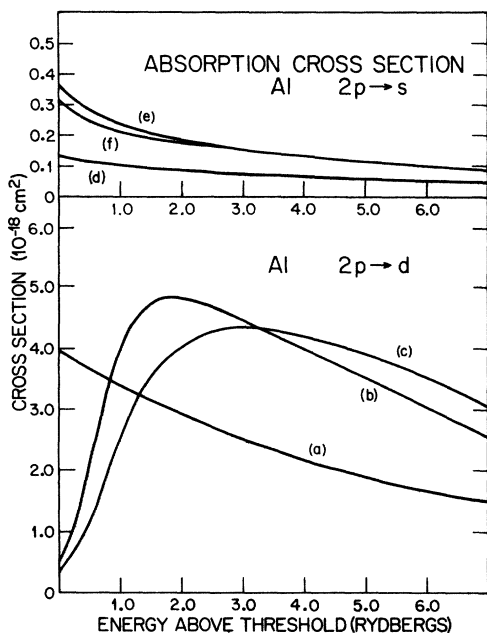


FIG. 5. $2p \rightarrow s$ and $2p \rightarrow d$ absorption cross section for Al: (a) $2p \rightarrow d$ free Al^{3+} ion absorption, (b) $2p \rightarrow d$ metallic Al absorption in normal approximation, (c) $2p \rightarrow d$ metallic Al absorption in sudden approximation, (d) $2p \rightarrow s$ free Al^{3+} ion absorption, (e) $2p \rightarrow s$ metallic Al absorption in normal approximation, and (f) $2p \rightarrow s$ metallic Al absorption in sudden approximation.

nant characteristics of the Na core hole s waves affect that solution.

One of our aims in this study was to calculate absorption and emission cross sections. Just as we did for free ions we calculated the single-particle cross sections in dipole approximation using the length form [see Eq. (4)]. We plot the $2p \rightarrow s$ and $2p \rightarrow d$ absorption transitions for Mg and Al in Figs. 4 and 5 and the $1s \rightarrow p$ absorption for Li in Fig. 6. Similar results were obtained for Na. We include cross sections calculated in the sudden approximation as well as the normal approximation. Note that the energy scale is in rydbergs. The same trends occur that were apparent for free ions. For a more attractive potential (Al rather than Mg) the $2p \rightarrow d$ cross section is larger near threshold because the radial-momentum matrix element is greater. For large energies the $2p \rightarrow d$ cross section becomes weaker for the more attractive potential in contradiction to the above argument. For large momenta, the valence wave functions have many nodes in the region where the bound-electron wave function is finite. The more attractive potential induces more nodes. Thus orthogonalization effects become important enough to decrease the cross section. The $2p \rightarrow s$ cross sections

for metals in the normal and sudden approximation also follow this trend. The contribution to the cross section changes drastically near threshold. In free ions the ratio σ of s -wave to d -wave cross section at threshold is 0.05 for Na^+ , 0.04 for Mg^{2+} , and 0.03 for Al^{3+} . The s -wave part is insignificant. In metals the ratio is 3.6 for Na, 1.6 for Mg, and 0.70 for Al. We get similar results using the sudden approximation. This is a confirmation of experimental observations that although d -wave contributions are more important for free ions, s -wave contributions can be equally important in metals. In fact, the x-ray edge divergences in Al, Mg, and Na are thought to be due to divergences in the s -wave cross section.

From Figs. 4–6 there is no reason to expect that either the sudden or normal approximation gives a better result for the absorption cross section. They both have the same form. In Figs. 7 and 8 we compare experimental results obtained from Deutsches Elektronen-Synchrotron (DESY) for x-ray absorption in Al and Mg (Ref. 33) with our results for both approximations. None of the calculated curves can produce the specific structure in the experimental curves—especially not the threshold divergences—but both agree qualitatively with the experimental observations. However Ritsko *et al.*²⁶ find that including backscattering as a correction to the one-electron results reproduces much of the structure away from threshold. The normal approximation gives better results near threshold. The sudden approximation is more accurate far from threshold. Low-energy outgoing electrons are slow enough that they stay near the core long enough to experience the relaxed potential. Higher-energy outgoing electrons spend less time near the core and are gone before the potential can relax. For

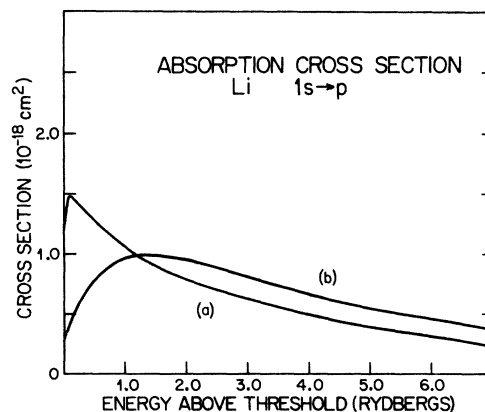


FIG. 6. $1s \rightarrow p$ absorption cross section for metallic Li: (a) in normal approximation, and (b) in sudden approximation.

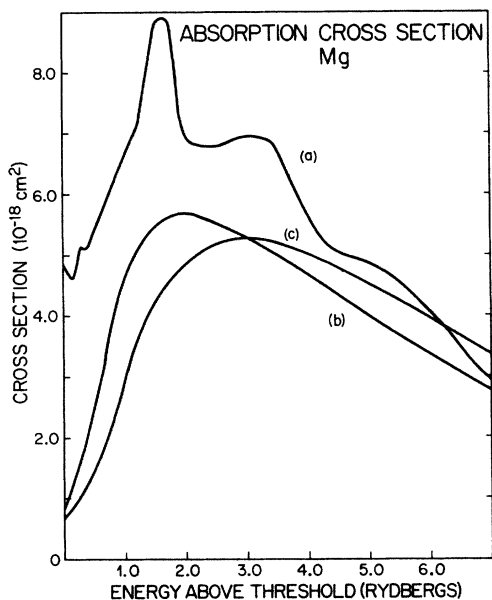


FIG. 7. Experimental and calculated total cross sections for metallic Mg: (a) experimental results of DESY (Ref. 33), (b) the normal approximation, and (c) the sudden approximation.

that reason the sudden approximation should be better at high energies and the normal approximation at low energies. However, the core hole should be screened in a time ω_p^{-1} . Since ω_p is

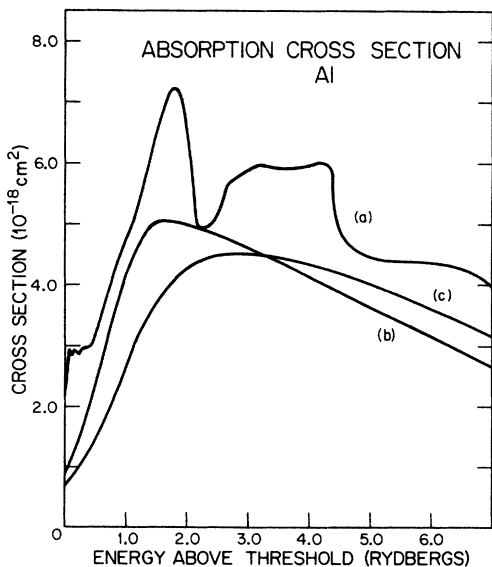


FIG. 8. Experimental and calculated total cross sections for metallic Al: (a) experimental results of DESY (Ref. 33), (b) the normal approximation, and (c) the sudden approximation.

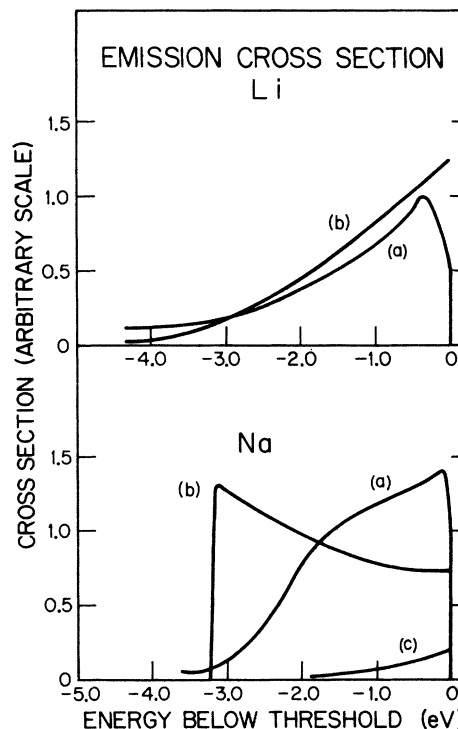


FIG. 9. Emission cross sections for Li and Na: (a) experimental results for Li (Ref. 29) and Na (Ref. 30), (b) $s \rightarrow 2p$ calculation for Na and $p \rightarrow 1s$ calculation for Li, and (c) $d \rightarrow 2p$ calculation for Na. By cross section we mean intensity divided by photon-frequency squared $[\nu(\omega)/\omega^2]$. The results have been scaled arbitrarily.

10^{15} sec^{-1} an electron with about the Fermi energy does not travel away from the core in that time. It is not clear which approximation is more appropriate.

We have also tried to calculate emission cross sections but with little success. In Figs. 9 and 10 we show calculated emission cross sections and experimental observations.^{29, 30} The experimental curves are scaled arbitrarily, relative to the calculated curves, so we can only compare the shapes. The obvious discrepancy is that there is a peak in the calculated curves for Na, Mg, and Al for energies near the bottom of the s -wave valence band which are not observed experimentally. This structure is similar to structure that is seen if a virtual bound state or resonance exists. As we mentioned earlier, results for Na indicate that there might be an s -wave bound state in the presence of a core hole. Matthew⁴⁹ has made measurements of double ionization satellites in Na that suggest that some valence states may be localized, however, experimental emission curves show no such behavior. We note that the results for Li show no peak. This confirms our result that the

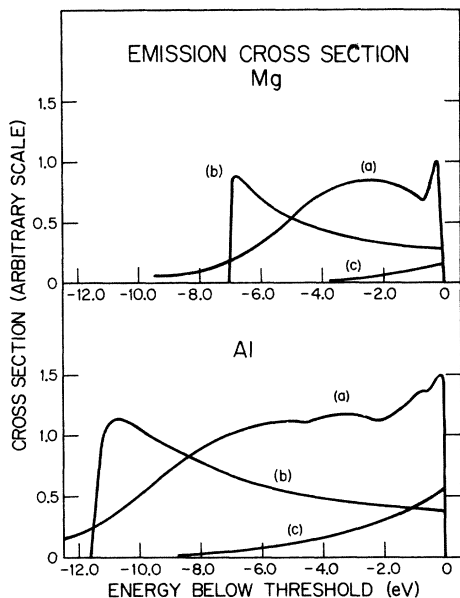


FIG. 10. Emission cross sections for Mg and Al: (a) experimental results for Mg (Ref. 30) and Al (Ref. 30), (b) $s \rightarrow 2p$ calculations, and (c) $d \rightarrow 2p$ calculations. By cross section, we mean intensity divided by photon-frequency squared $[(\omega)/\omega^2]$. The results have been scaled arbitrarily.

p -wave phase shift at zero wave vector is zero for Li.

We also test the explanation by Mahan,³⁴ Nozières and de Dominicis³⁵ using many-body theory of the threshold singularities observed in soft-x-ray spectra. We test this by using phase shifts obtained from our model to calculate the predicted threshold exponents. Nozières and de Dominicis predict that near threshold, emission and absorption have the form

$$\sigma_{i \rightarrow i \pm 1}(\epsilon) = C [(\epsilon - \epsilon_{th})/\xi]^{\alpha_{i \pm 1}},$$

where ϵ_{th} is the threshold energy and ξ a cutoff

energy. They predict that

$$\alpha_l = (2/\pi)\eta_l(\epsilon_F) - \alpha,$$

$$\alpha = 2 \sum_l (2l+1) \left(\frac{\eta_l(\epsilon_F)}{\pi} \right)^2,$$

where $\eta_l(\epsilon_F)$ is the phase shift for an electron with angular momentum l and energy ϵ_F moving in the potential of the core hole. Almbladh and von Barth²⁴ show that this phase shift is the difference in phase shifts calculated for scattering off the potentials for the metal with and without a core hole. We present our calculations in Table VI as well as those of Almbladh and von Barth and experimental results for α_0 obtained from an empirical fit done by Dow and Sonntag³⁷ and experimental results for α obtained from XPS measurements done recently by Citrin, Wertheim, and Baer.^{39, 40} We get very poor results for Na because the core-hole phase shifts are very big due to the apparent s -wave bound-valence state. However we get much better results for Li, Mg, and Al. Our results for α_0 agree much better with the experimental fit of Dow than do the results of Almbladh. We also get good agreement with experiment for the α of Li, Mg, and Al. Our results for the α of Mg and Al are within the allowed range of values determined by Citrin. Our value of α for Li falls just outside the allowed range of values. Our results for α_1 do not agree with the results of Neddermeyer.³⁸ However he attributes a large error to his result for Al so our disagreement is not significant.

V. SUMMARY

We have presented a model of a metal in which an ion is placed at the center of a jellium metal. A spherical hole in the background is taken out around the ion and the core and valence electrons relax into a self-consistent solution. We do this for states with and without a core hole. We have

TABLE VI. The threshold exponents α , α_0 , and α_1 for (a) this work, (b) Almbladh and von Barth, and (c) experimental results.

	α^a	α_0^a	α_1^a	α^b	α_0^b	α_1^b	α^c	α_0^c	α_1^c
Li	0.16	0.23	0.08	0.16	0.27	0.05	0.23 ^a	0.22 ^b	...
Na	0.54	0.10	-0.10	0.20	0.38	-0.05	0.20 ^a	0.27 ^b	...
Mg	0.12	0.19	0.10	0.13 ^a	0.23 ^b	-0.01 ^c
Al	0.10	0.13	0.12	0.13	0.06	0.14	0.12 ^a	0.14 ^b	0.02 ^c

^a From P. H. Citrin, G. K. Wertheim, and Y. Baer (Refs. 39 and 40).

^b From the fit of Dow and Sonntag (Ref. 37).

^c From H. Neddermeyer (Ref. 38).

tested this model by studying the free ion photoionization of Ne, Na⁺, Mg²⁺, and Al³⁺. We get the best agreement with experiment when we eliminate bound electron self-interaction effects from our single-particle potential. When we test this model by studying metallic Li, Na, Mg, and Al we get self-consistent solutions that obey the Friedel sum rule to five decimal places. We predict threshold energies and power-law exponents for each metal. We get very satisfactory results for every metal but Na. This failure for Na is caused by the anomalous behavior of the *2p* core-hole solution for Na. We also calculate absorption and emission cross sections for each metal. The absorption cross sections for Mg and Al agree qualitatively with measured cross sections—but without the band-structure effects and the many-body enhancement. Our emission cross sections show low-energy peaks indicative of the resonance behavior we have seen in our solution for Na.

Recently Flynn⁵⁰ has made measurements on the optical absorption of halides in alkalis. Their results seem to be incompatible with MND theory. They find large negative values for α_0 . It would be interesting to test this with our model. Not only can we study the impurity problem with our model, but we can extend it to study deep-core-hole states. Feibelman and McGuire⁵¹ made a simple

1-OPW calculation of Na *KLV* Auger line shapes to see if matrix-element effects would explain the “mystery” peaks measured by Barrie and Street.⁵² Our model would be an ideal starting point from which to obtain realistic wave functions needed to study these matrix-element effects.

Note added in proof. Our calculations show a weak bound state for Na²⁺ in sodium metal. If such a state exists, then according to the theory of M. Combescot and P. Nozières, *J. Phys. (Paris)* **32**, 913 (1971), the edge spectra should be calculated with the bound state occupied. We did not do this, which could explain the poor results. In fact, our calculations would describe the secondary threshold they predict. However, it is more likely that this bound state is an artifact of the model. The use of a more realistic potential with periodic centers of attraction should delocalize this weakly bound state. Recently G. Wertheim and P. Citrin, “Fermi Surface Excitations in X-Ray Photoemission Lineshapes from Metals” in *Photoemission in Solids* (unpublished), reanalyzed the x-ray edge data for Al. Our value for α_1 for Al is consistent with their new experimental value of $\alpha_1 = 0.095$.

ACKNOWLEDGMENT

This research was supported by the NSF.

-
- ¹P. Hohenberg and W. Kohn, *Phys. Rev.* **136**, B864 (1964).
²N. D. Lang, *Solid State Phys.* **28**, 225 (1973).
³W. Kohn and L. J. Sham, *Phys. Rev.* **140**, A1133 (1965).
⁴H. Bethe and R. Jackiw, *Intermediate Quantum Mechanics* (Benjamin, Reading, Mass., 1968).
⁵F. Herman and S. Skillman, *Atomic Structure Calculations* (Prentice-Hall, Englewood Cliffs, N.J., 1962).
⁶B. Y. Tong and L. J. Sham, *Phys. Rev.* **144**, 1 (1966).
⁷R. D. Cowan, A. Larson, D. Liberman, J. B. Mann; and J. Waber, *Phys. Rev.* **144**, 5 (1966).
⁸I. Lindgren, *Phys. Lett.* **19**, 382 (1965).
⁹S. T. Manson and J. W. Cooper, *Phys. Rev.* **165**, 126 (1968).
¹⁰F. Combet Farnoux and M. Lamoureux, *J. Phys.* **B 9**, 897 (1976).
¹¹E. J. McGuire, *Phys. Rev.* **175**, 20 (1968).
¹²J. D. W. Connolly, *Phys. Rev.* **159**, 416 (1967).
¹³P. De Cicco, *Phys. Rev.* **153**, 931 (1967).
¹⁴W. E. Rudge, *Phys. Rev.* **181**, 1024 (1969).
¹⁵M. Ross and K. W. Johnson, *Phys. Rev. B* **2**, 4709 (1970).
¹⁶P. M. Marcus, J. F. Janak, and A. R. Williams, *Computational Methods in Band Theory* (Plenum, New York, 1971).
¹⁷B. Y. Tong, *Phys. Rev. B* **6**, 1189 (1972).
¹⁸L. Dagens, *J. Phys. C* **5**, 2333 (1972).
¹⁹C. O. Almbladh, U. von Barth, Z. D. Popovic, and M. J. Stott, *Phys. Rev. B* **14**, 2250 (1976).
²⁰E. Zaremba, L. M. Sander, and H. B. Shore, and J. H. Rose (unpublished).
²¹N. D. Lang and W. Kohn, *Phys. Rev. B* **1**, 4555 (1970).
²²N. D. Lang and W. Kohn, *Phys. Rev. B* **3**, 1215 (1971).
²³K. H. Lau and W. Kohn, *J. Phys. Chem. Solids* **37**, 99 (1976).
²⁴C. O. Almbladh and U. von Barth, *Phys. Rev. B* **13**, 3307 (1976).
²⁵C. P. Flynn and N. O. Lopari, *Phys. Rev. B* **7**, 2215 (1973).
²⁶J. J. Ritsko, S. E. Schnatterly, and P. C. Gibbons, *Phys. Rev. Lett.* **32**, 671 (1974).
²⁷R. P. Gupta and A. J. Freeman, *Phys. Rev. Lett.* **36**, 1194 (1976).
²⁸L. Smrcka, *Czech. J. Phys. B* **21**, 683 (1971).
²⁹D. J. Fabian, *Soft X-Ray Band Structure* (Academic, New York, 1968).
³⁰*Electronic Density of States*, edited by L. H. Bennett, Natl. Bur. Stand., Spec. Publ. No. 323 (U.S. GPO, Washington, D. C., 1971).
³¹R. Haensel, G. Keitel, B. Sonntag, C. Kunz, and P. Schreiber, *Phys. Status Solidi A* **2**, 85 (1970).
³²R. Haensel, G. Keitel, P. Schreiber, B. Sonntag, and C. Kunz, *Phys. Rev. Lett.* **23**, 528 (1969).
³³H. J. Hagemann, W. Gudat, and C. Kunz, *Optical Constants from the Far Infrared to the X-ray Region: Mg, Al, Cu, Ag, Au, Bi, C and Al₂O₃*, DESY SR-7417 (Desy, Hamburg, W. Germany, 1974).
³⁴G. D. Mahan, *Phys. Rev.* **153**, 882 (1967); **163**, 612

- (1967).
- ³⁵P. Nozières and C. T. de Dominicis, *Phys. Rev.* 178, 1097 (1969).
- ³⁶S. Doniach and M. Sunjić, *J. Phys. C* 3, 285 (1970).
- ³⁷J. Dow and B. Sonntag, *Phys. Rev. Lett.* 31, 1132 (1973).
- ³⁸H. Neddermeyer, *Phys. Rev. B* 6, 2411 (1976).
- ³⁹P. Citrin, G. Wertheim, and Y. Baer, *Phys. Rev. Lett.* 35, 49 (1976).
- ⁴⁰P. Citrin, G. Wertheim, and Y. Baer (unpublished).
- ⁴¹E. Wigner, *Phys. Rev.* 46, 1002 (1934).
- ⁴²R. D. Cowan, *Phys. Rev.* 163, 54 (1967).
- ⁴³J. Samson, *J. Opt. Soc. Am.* 55, 935 (1965).
- ⁴⁴R. J. W. Henry and L. Lipsky, *Phys. Rev.* 153, 51 (1967).
- ⁴⁵C. E. Moore, *Atomic Energy Levels*, Natl. Bur. Stand. Circ. No. 467 (U.S. GPO, Washington, D.C., 1949), Vol. 1.
- ⁴⁶L. I. Schiff, *Quantum Mechanics* (McGraw-Hill, New York, 1968).
- ⁴⁷J. A. Bearden and A. F. Burr, *Rev. Mod. Phys.* 39, 125 (1967).
- ⁴⁸J. F. Friedel, *Nuovo Cimento Suppl.* 7, 287 (1958).
- ⁴⁹J. A. D. Matthew, *Phys. Lett. A* 50, 401 (1975).
- ⁵⁰D. J. Phelps, R. A. Tilton, and C. P. Flynn, *Phys. Rev. B* 14, 5254 (1976).
- ⁵¹P. J. Feibelman and E. J. McGuire, *Phys. Rev. B* 6, 3006 (1977).
- ⁵²A. Barrie and F. J. Street, *J. Electron Spectrosc. Relat. Phenom.* 7, 1 (1975).